Electrocatalysis (2014) 5:438–444
DOI 10.1007/s12678-014-0213-2

Electrochemical and Fuel Cell Evaluation of PtIr/C Electrocatalysts for Ethanol Electrooxidation in Alkaline Medium

Sirlane G. da Silva · Mônica H. M. T. Assumpção · Rodrigo F. B. de Souza · Guilherme S. Buzzo · Estevam V. Spinacé · Almir O. Neto · Júlio César M. Silva

Published online: 21 June 2014

Abstract PtIr/C electrocatalysts prepared by borohydride reduction process were characterized by X-ray diffraction, transmission electron microscopy, and cyclic voltammetry. The X-ray diffraction measurements suggested the PtIr alloy formation; furthermore, peaks of IrO_2 were not observed; nevertheless, the presence of Ir oxides in small amounts and amorphous forms cannot be discarded. The transmission electron microscopy showed the average particle diameter between 4.0 and 6.0 nm for all compositions prepared. The catalytic activity for ethanol electrooxidation in alkaline medium at room temperature (cyclic voltammetry and chronoamperometry results) showed that PtIr/C (70:30) and PtIr (90:10) exhibited higher performance toward ethanol oxidation than the other electrocatalysts. Experiments using direct ethanol alkaline fuel cell at 75 °C showed PtIr (90:10) as the best electrocatalyst and Ir/C as virtually inactive for ethanol oxidation in real conditions. The best result obtained using PtIr/C may be associated to the electronic effect between Pt and Ir that could decrease the poisoning on catalyst surface and also by the occurrence of bifunctional mechanism.

Keywords Direct ethanol alkaline fuel cell · PtIr/C · Electrocatalysts

Introduction

Alkaline direct liquid fuel cells (ADLFC) have recently attracted worldwide attention, because they are low-cost and show promise as clean and efficient power sources. The use of a ADLFC also shows advantages in comparison with proton exchange membrane fuel cells (PEMFC), since the kinetics of the oxygen reduction reaction (ORR) is more facile and the less corrosive nature of an alkaline environment ensures a potential greater longevity [1–3].

Ethanol has been considered one of the most promising candidates for ADLFC, because it could be produced in a large scale from renewable sources, which will not change the natural balance of carbon dioxide in the atmosphere in contrast to the use of fossil fuels; moreover, it is less toxic than other liquid combustible [4, 5]. However, the high efficiency of the ethanol oxidation reaction (EOR) is still a significant goal because the cleavage of C–C bonds for the complete oxidation of ethanol to CO_2 requires the use of more active and selective anode catalysts [5].

Platinum or palladium are generally used as electrocatalysts for the ethanol oxidation in acidic or alkaline media environment; however, the activity of Pt or Pd for ethanol oxidation in alkaline media needs to be enhanced due to the difficulty in breaking the C–C bond and to the formation of intermediates that poison Pt/C or Pd/C anodes, reducing the fuel cell performance [6]. An alternative is the addition of co-catalysts to Pt or Pd electrocatalysts [6–8] such as gold whose electrocatalytic activity in alkaline media is greater than in acid media [9].

According to da Silva et al. [10], the improvement in ethanol oxidation on gold in alkaline medium is related to the fact that practically no poisoning species (CO-like species) can be formed and adsorbed on the surface [10]. Moreover, PtAu/C electrocatalysts prepared by the conventional borohydride reduction method have enhanced activity for methanol oxidation in comparison to Pt/C electrocatalysts [11]. Also, Jin et al. [12] showed that PtAu/C electrocatalysts have high activity and stability in alkaline solution for ethylene glycol oxidation.

On the other hand, the incorporation of Ir or IrO_2 on Pt (PtIr or $PtIrO_2$) has also improved the catalytic activity and stability

S. G. da Silva · M. H. M. T. Assumpção · R. F. B. de Souza · G. S. Buzzo · E. V. Spinacé · A. O. Neto (✉) · J. C. M. Silva
Instituto de Pesquisas Energéticas e Nucleares, IPEN/CNEN-SP, Av. Prof. Lineu Prestes, 2242 Cidade Universitária, São Paulo, SP CEP 05508-900, Brazil
e-mail: aolivei@ipen.br

of catalysts for ethanol oxidation in acid media [13, 14]. This improvement was attributed to the hydroxyl groups which are more easily adsorbed on both metallic Ir or iridium oxide (IrO_2) at lower potentials, assisting in the oxidation of adsorbed intermediates [15].

Xu et al. [16] prepared bimetallic PdIr electrocatalysts, where the addition of Ir to Pd improved the ethanol oxidation kinetics in comparison with pure Pd in alkaline media. The Pd_7Ir/C electrocatalyst exhibited higher activity and stability than the other samples. The improvement in catalytic performance was attributed to Ir addition to Pd electrocatalyst which could facilitate the removal of adsorbed ethoxi intermediates.

In alkaline media, Pd-based electrocatalysts [1, 2] seems to be superior to Pt-based catalysts in terms of activity for ethanol oxidation and poison tolerance; however, more information about Pt-based catalysts using a direct alkaline ethanol fuel cell are necessary. Thus, this work describes the use of PtIr/C electrocatalysts, prepared in different Pt/Ir atomic ratios, for the ethanol oxidation reaction in alkaline media. This work includes both electrochemical (cyclic voltammetry and chronoamperometry) and single cell experiments (real conditions of operation). The single cell experiments were realized with KOH-modified Nafion112 membrane as already proposed by Sun et al. [17].

Experimental

PtIr/C electrocatalysts (with 20 % *w*/*w* and Pt/Ir atomic ratios of 90:10, 80:20, 70:30, and 50:50) were prepared by borohydride reduction using $H_2PtCl_6 \cdot 6H_2O$ and $IrCl_3$ as metal sources, Vulcan XC72 as support, and sodium borohydride as reducing agent. In this method, the Vulcan XC72 was firstly dispersed in an isopropyl alcohol/water solution (50:50, *v*/*v*); after that, the mixture resulting was homogenized under stirring and then the metal sources were added and put on an ultrasonic bath for 5 min. Finally, a solution of sodium borohydride into 0.1 mol L^{-1} KOH was added in one portion under stirring at room temperature and the resulting solution was maintained under stirring for more 15 min. After that, the final mixture was filtered and the solids washed with water and then dried at 70 °C for 2 h.

PtIr/C electrocatalysts were characterized by XRD analyses using a Rigaku diffractometer model Miniflex II using Cu Kα radiation source (λ=0.15406 nm). The diffractograms were recorded from 2θ=20° to 90° with a step size of 0.05° and a scan time of 2 s per step. TEM analyses were also carried out using a JEOL JEM-2100 electron microscope operated at 200 kV, where the morphology, distribution, and size of the nanoparticles in the support were determined. The mean particle sizes were determined by counting more than 100 particles from different regions of each sample [18]. The atomic ratios of Pt and Ir in the synthesized materials were measured by energy dispersive spectroscopy (EDS) by using JEOL JSM-6010 LA equipment.

A potentiostat/galvanostat PGSTAT30 was employed for the electrochemical measurements, where a conventional three-electrode electrochemical cell was used. A platinum electrode and an Ag/AgCl (3 mol L^{-1} KCL) were used as the counter and reference electrodes, respectively. The work electrodes (geometric area of 0.5 cm^2 with a depth of 0.3 mm) were prepared using the thin porous coating technique [19]. The initial characterizations were made using cyclic voltammetry (CV), where all the cyclic voltammograms illustrated were obtained after ten cycles. These experiments were conducted at a scan rate of 10 mV s^{-1} in 1 mol L^{-1} KOH aqueous solution in the presence and absence of 1 mol L^{-1} ethanol. The amperometric curves (I–T) were recorded in the same electrolyte containing ethanol at −0.35 V for 1,800 s.

The direct ethanol alkaline fuel cell took place in a single cell with an area of 5 cm^2. The temperature was set to 75 °C for the fuel cell and 85 °C for the oxygen humidifier. All electrodes used contained 1 mg of Pt per square centimeter in the anode and in the cathode, except for Ir/C which contained 1 mg of Ir per square centimeter. In all experiments, Pt/C BASF was used in the cathode. The electrocatalyst was painted over a carbon cloth in the form of a homogeneous dispersion prepared using Nafion® solution (5 wt%, Aldrich) in relation to 30 % catalyst/polymer (*w*/*w*). After the preparation, the electrodes were hot pressed on both sides of a Nafion® 117 membrane at 125 °C for 3 min under a pressure of 100 kgf cm^{-2}. Prior to use, the membranes were exposed to KOH 6 mol L^{-1} for 24 h. The experiments were realized in the

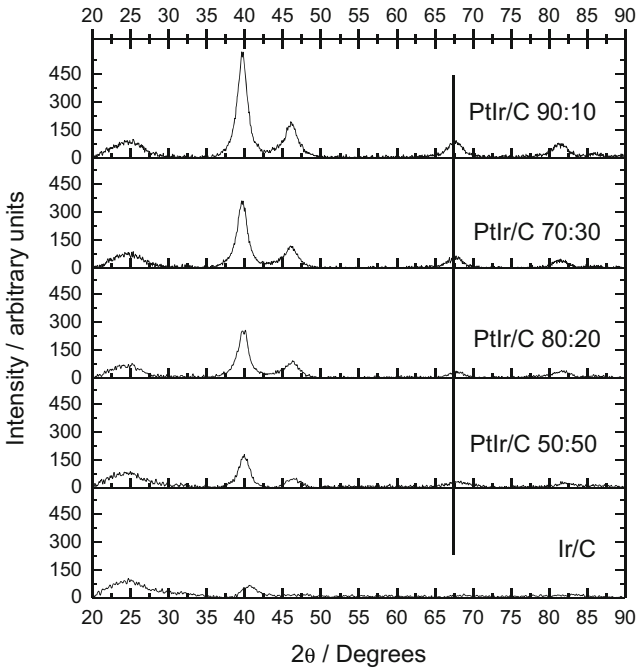

Fig. 1 X-ray diffraction patterns for the Ir/C and PtIr/C electrocatalysts prepared with atomic ratios of 90:10, 80:20, 70:30, and 50:50

presence of 2.0 mol L^{-1} C_2H_5OH and 2.0 mol L^{-1} KOH. The fuel was delivered at 2.0 mL min^{-1} and the oxygen flow was regulated at 150 mL min^{-1}. Polarization curves were obtained by using a potentiostat/galvanostat PGSTAT 302 N Autolab.

Results and Discussion

The X-ray diffractograms of the PtIr/C and Ir/C electrocatalysts are shown in Fig. 1. All PtIr/C diffractograms showed four peaks in 2θ=40°, 47°, 67°, and 82°, which are associated with the 111, 200, 220, and 311 planes, characteristic of Pt face-centered cubic (fcc) structure and a broad peak at about 25° associated with Vulcan XC72 support. For PtIr/C was not observed, the peak characteristics of IrO_2 at 34.5° and 54° PtIr/C alloy showed that the positions of 220 crystalline plane are shifted to high values compared to 67° for Pt [13, 14]. This result is in accord with the work of Tremiliosi-Filho [20]; these authors observed that the binary PtIr electrocatalysts shift the reflection planes to higher 2θ values and no phase separation occurs, consequently this behavior suggested the formation of a solid solution between Pt and Ir. The experimental compositions of all PtIr/C materials using the EDS analysis were 89:11 (nominal 90:10), 79:21 (nominal 80:20), 68:32 (nominal 70:30), and 53:47 (nominal 50:50). As can be seen, the percentage of each metal is close to nominal values in all cases.

TEM micrographs and histograms of particle mean diameter distribution for the PtIr/C and Ir/C electrocatalysts are shown in Fig. 2. All electrocatalysts prepared showed the particles well-

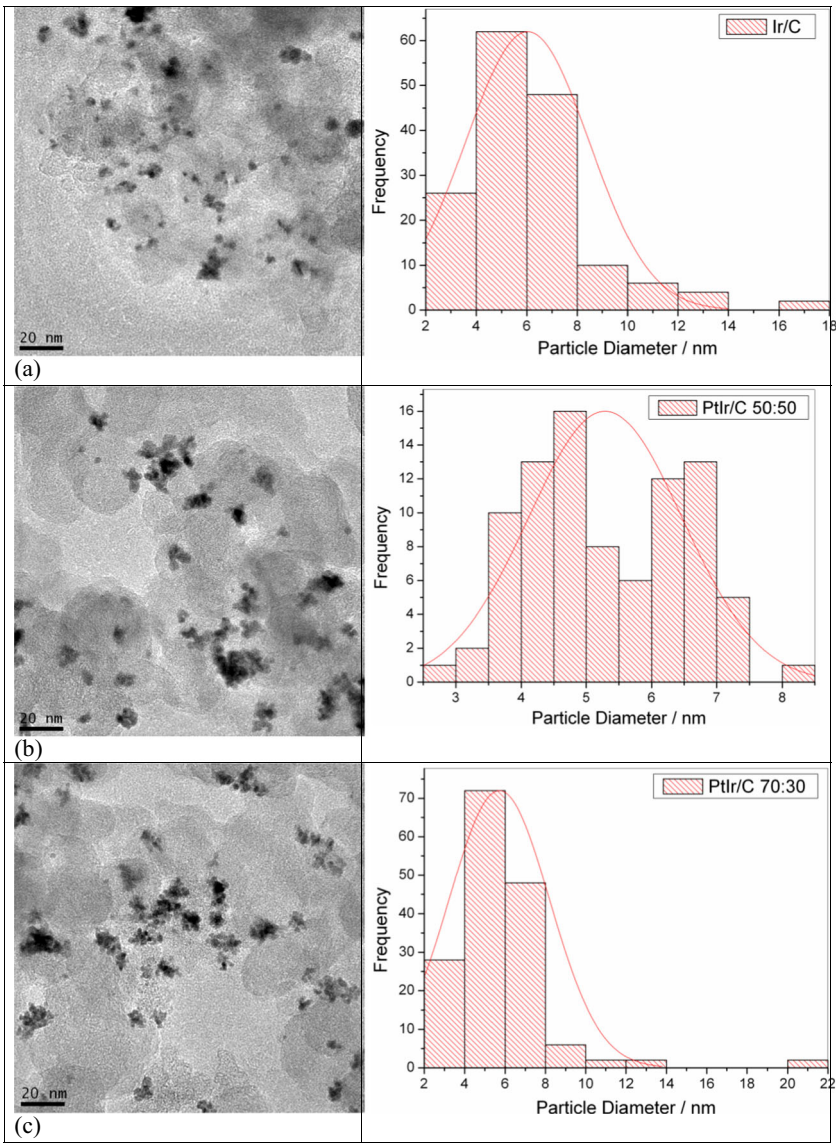

Fig. 2 TEM micrographs and histograms of the particle size distribution of **a** Ir/C, **b** PtIr/C (50:50), **c** PtIr/C (70:30), **d** PtIr/C (80:20), and **e** PtIr/C (90:10)

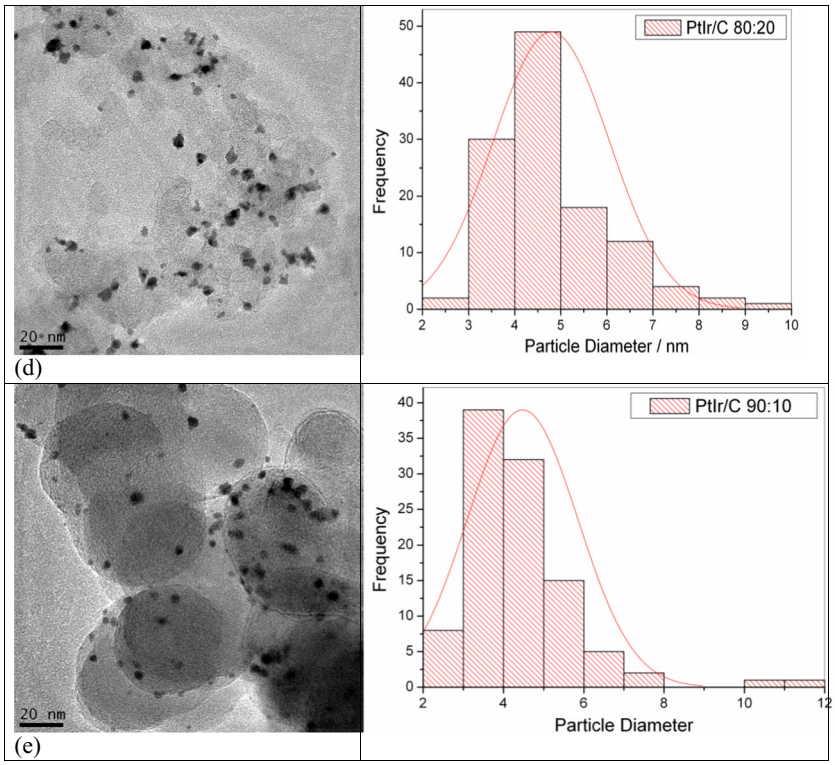

Fig. 2 (continued)

dispersed on carbon support, although some small particle agglomerations can be seen for PtIr/C (70:30) and PtIr/C (80:20). The mean particle sizes for Ir/C, PtIr/C (50:50), PtIr/C (70:30), PtIr/C (80:20), and PtIr/C (90:10) were 6.0, 5.3, 5.7, 4.8, and 4.5 nm, respectively. Only Ir/C and PtIr/C 70:30 showed a small percentage of particles higher than 10 nm, with a maximum mean diameter of 20 and 16 nm, respectively. The same behavior has been observed by Ribeiro et al. [20] and Basu [14] for PtIr (75:25) and PtIr (50:50). These electrocatalysts showed particle sizes lying between 2 and 8 nm with large agglomerates with sizes between 10 and 15 nm. These authors concluded that the agglomeration could be associated to the fast reduction in the synthesis process.

The cyclic voltammograms of Ir/C, PtIr/C (50:50), PtIr/C (70:30), PtIr/C (80:20), and PtIr/C (90:10) in presence of 1.0 mol L^{-1} KOH solution are shown in Fig. 3. PtIr/C voltammograms do not display a well-defined hydrogen oxidation region (−0.85 to −0.60 V versus Ag/AgCl) in comparison to pure platinum.

The current densities in the double layer region of PtIr/C (between −0.55 and −0.2 V versus Ag/AgCl) are larger than those in pure platinum. This behavior is characteristic of binary and ternary electrocatalysts containing transition metals and it can be explained by a better material dispersion on carbon and/or the formation of ultrafine particles [20].

The voltammograms of all PtIr/C electrocatalysts are also suppressed in comparison with Pt/C, indicating partial coverage of Pt by Ir or a formation of iridium oxides. The hydrogen adsorption did not occur on Ir surface once that the hydrogen adsorption–desorption region is suppressed in Ir/C electrocatalyst.

Figure 4 shows the CV of Pt/C, PtIr/C (50:50), PtIr/C (70:30), PtIr/C (80:20), PtIr/C (90:10), and Ir/C in the presence of 1.0 mol L^{-1} of ethanol and in 1.0 mol L^{-1} KOH with a scan rate of 10 mV s^{-1}. The CVs were normalized per gram of Pt and Ir.

On a potential of −0.35 V (interest application fuel cell), PtIr/C (90:10), PtIr/C (70:30), and PtIr/C (50:50) showed the

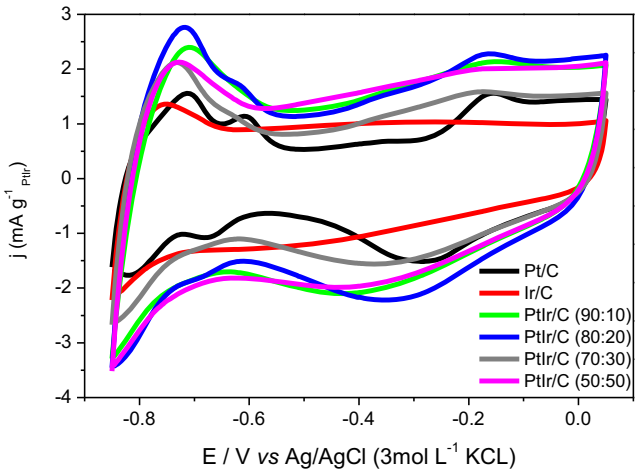

Fig 3 Cyclic voltammograms of Pt/C, PtIr/C (50:50), PtIr/C (70:30), PtIr/C (80:20), PtIr/C (90:10), and Ir/C in the presence of 1.0 mol L^{-1} KOH with a scan rate of 10 mV s^{-1}

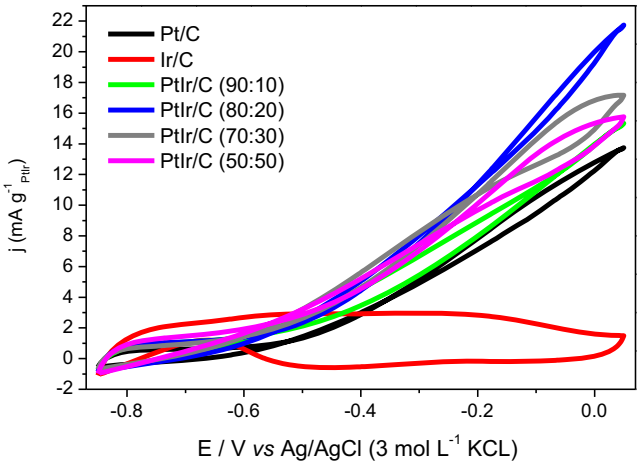

Fig 4 Cyclic voltammograms of Pt/C, PtIr/C (50:50), PtIr/C (70:30), PtIr/C (80:20), PtIr/C (90:10), and Ir/C in the presence of 1.0 mol L^{-1} KOH and 1.0 mol L^{-1} of ethanol with a scan rate of 10 mV s^{-1}

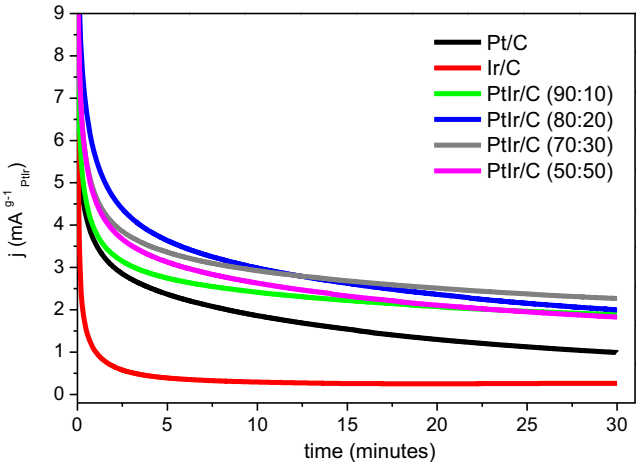

Fig 5 Current–time curves at −0.35 V in 1 mol L^{-1} ethanol solution and 1.0 mol L^{-1} KOH for Pt/C, PtIr/C (50:50), PtIr/C (70:30), PtIr/C (80:20), PtIr/C (90:10), and Ir/C at 25 °C

best performance toward ethanol electrooxidation in comparison with PtIr/C (80:20) and Pt/C electrocatalysts. The ethanol oxidation starts at a potential of about −0.65 V for PtIr electrodes vs around −0.55 V for the Pt/C. Pt/C showed the lowest performance, consequence of the lowest current values observed in relation to PtIr/C electrocatalysts, while Ir/C electrocatalyst was virtually inactive toward ethanol oxidation.

Xu et al. [16] showed that the introduction of Ir leads to an increase in the electro-activity of the binary electrocatalysts (PdIr) compared to pure Pd. This effect was explained by the activation of interfacial water molecules at lower potentials than in the case of pure Pd, due to the presence of preferential sites for OH_{ads} adsorption. The presence of OH_{ads} species, necessary for the complete oxidation of poisoning intermediates adsorbed, associated with the electronic modification of Pd might be the possible reason for the enhanced activity. Thus, the addition of Ir to Pt might have a similar effect of the one observed on Pd. Moreover, it is known that the introduction of Ir to Pt improves the ethanol oxidation in acid medium [14, 20, 21].

Figure 5 shows the chronoamperometry curves for Pt/C, PtIr/C (50:50), PtIr/C (70:30), PtIr/C (80:20), PtIr/C (90:10), and Ir/C in the presence of 1.0 mol L^{-1} KOH and 1.0 mol L^{-1} of ethanol in the potential of −0.35 V for 30 min. It is possible to observe for all PtIr/C and Pt/C electrocatalysts a faster decay of current during the first minutes followed by a slower decay. The final current values at −0.35 V were as follows: PtIr/C (70:30)>PtIr/C (90:10)>PtIr/C (80:20)~PtIr/C (50:50)>Pt/C>Ir/C. The current density measured for PtIr/C (70:30) is about 2.3 times higher than that obtained with Pt/C. These results indicate that the introduction of 10–30 % of Ir in Pt catalysts results in improvement in ethanol oxidation. The optimal composition is commonly attributed as required for the bifunctional mechanism occurrence and the electronic effect. Additionally, the optimal composition depends on the electrocatalysts preparation method [13]. This occurs because there are differences between shapes, phases, dispersions, morphologies, and superficial phases, and these parameters can contribute either high or low coverage of the adsorption sites within the oxide [22, 23].

Xu et al. [16] showed that Pd_7Ir/C catalyst had a lower polarization potential than Pd/C, and with the increase in time,

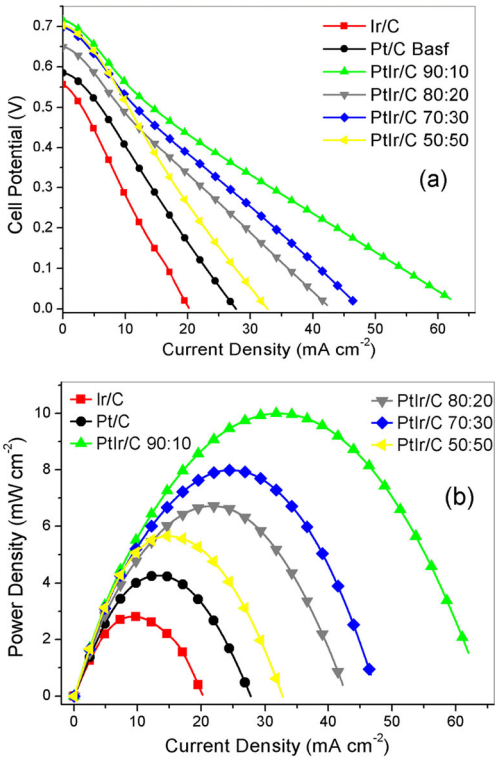

Fig 6 Direct ethanol fuel cell performance of Pt/C, PtIr/C (50:50), PtIr/C (70:30), PtIr/C (80:20), PtIr/C (90:10), and Ir/C electrocatalysts, where I–V curves (**a**) and the power density (**b**) were obtained at 75 °C in 5 cm^2

the potential difference becomes larger, indicating that Ir addition to Pd could facilitate the removal of the adsorbed ethoxi intermediates, hence releasing more active Pd sites for the EOR and making it more resistant to poisoning. However, this author concluded that for the enhancement in the catalytic performance of the PdIr catalysts, studies are further needed to separate the contribution from metallic Ir and IrO_2.

Then, the best results obtained on chronoamperometry measurements using PtIr/C compared to Pt/C might be associated to a disturbance at the Pt orbital symmetries caused by iridium atoms, thereby affecting the ethanol adsorption and, consequently, the electrooxidation rate, additionally promoting a lower poisoning of adsorbed species, as recently proposed for PtIr/C and IrPtSn/C in case of ethanol oxidation in acid medium [13, 14, 20].

Figure 6 shows the performances of a single direct ethanol fuel cell (DAEFC) operating at 75 °C with PtIr/C (50:50), PtIr/C (70:30), PtIr/C (80:20), PtIr/C (90:10), and Ir/C as anode electrocatalysts and Pt/C BASF as cathode in all experiments.

It was possible to be observed that the open circuit voltage of the fuel cell for PtIr/C (50:50), PtIr/C (70:30), PtIr/C (80:20), PtIr/C (90:10), Ir/C, and Pt/C were 0.70, 0.69, 0.65, 0.72, 0.56, and 0.59, respectively. However, PtIr/C (90:10) electrocatalyst showed higher values of maximum power density (10 mW cm^{-2}) in comparison with PtIr/C (70:30, 8 mW cm^{-2}), PtIr/C (80:20, 6.5 mW cm^{-2}), PtIr/C (50:50, 5.5 mW cm^{-2}), Pt/C (4.5 mW cm^{-2}), and Ir/C (2.5 mW cm^{-2}). The experiments at 75 °C on single DAEFC showed that the power density for PtIr/C (90:10) was 2.5 times higher that ones obtained using Pt/C.

The result on single ethanol fuel cell shows the PtIr/C (90:10) as the best binary composition in comparison with other PtIr/C and Pt/C electrocatalysts. This behavior might be associated to the anode construction, where the Pt load is constant (1 mg_{Pt} cm^{-1}), consequently, the anode composed of PtIr/C (70:30) and PtIr (50:50) is thicker than the PtIr/C (90:10), yielding also more resistive electrode what difficult the fuel diffusion through the catalytic layer. Moreover, it is known that the electrical resistance and the ability of the fuel in diffusing through the MEA are factors that strongly influence the fuel cell efficiency [24–27]. Thus, the better results obtained using PtIr/C binary composition compared to Pt/C and Ir/C might be associated with the effect generated between Pt and Ir in close contact (alloy) and bifunctional mechanism.

Assumpção et al. [28] studied a direct ethanol fuel cell using PtAu/C as anodes in similar conditions with this work. In this work, PtAu/C 70:30 was the best material toward ethanol electrooxidation in comparison with Pt/C and other PtAu/C prepared. PtAu/C 70:30 also showed a power density three times higher than the one obtained using Pt/C. These authors concluded that the best result obtained with PtAu/C might be associated with the effect generated between Pt and Au in close contact (alloy) that contributes to the C–C cleavage.

Conclusion

The borohydride reduction process showed to be an effective method to produce PtIr/C electrocatalysts in a single step. This method yields electrocatalysts with mean particle size between 4.0 and 6.0 nm for all prepared materials. PtIr/C diffractograms showed peaks characteristic of Pt face-centered cubic (fcc) and the formation of an alloy between Pt and Ir.

All PtIr/C exhibited higher performance for ethanol oxidation in alkaline media when compared to Pt/C at room temperature. The best results obtained using PtIr/C may be associated with the effect generated between Pt and Ir in close contact (alloy) and also by the bifunctional mechanism (oxygen species observed in the cyclic voltammetry). However, further work is now necessary to investigate the electrocatalyst surface in order to elucidate the mechanism of ethanol electrooxidation using these electrocatalysts.

Acknowledgments The authors wish to thank FAPESP (2013/01577-0, 2011/18246-0, 2012/22731-4, 2012/03516-5) and CNPq (150639/2013-9) for the financial support.

References

1. E. Antolini, E.R. Gonzalez, J. Power Sources **195**, 3431–3450 (2010)
2. E. Antolini, J. Power Sources **170**, 1–12 (2007)
3. M.M. Tusi, N.S.O. Polanco, S.G. da Silva, E.V. Spinacé, A.O. Neto, Electrochem. Commun. **13**, 143–146 (2011)
4. S.Y. Shen, T.S. Zhao, J.B. Xu, Int. J. Hydrog. Energy **35**, 12911–12917 (2011)
5. H. Wendt, E.V. Spinace, A.O. Neto, M. Linardi, Quim. Nova **28**, 1066–1075 (2011)
6. A. Dutta, S.S. Mahapatra, J. Datta, Int. J. Hydrog. Energy **36**, 14898–14906 (2011)
7. C. Xu, P.K. Shen, J. Power Sources **142**, 27–29 (2005)
8. Y. Huang, J. Cai, Y. Guo, Appl. Catal. B Environ. **129**, 549–555 (2013)
9. G. Tremiliosi-Filho, E.R. Gonzalez, A.J. Motheo, E.M. Belgsir, J.M. Léger, C. Lamy, J. Electroanal. Chem. **444**, 31–39 (1998)
10. D.F. da Silva, A.N. Geraldes, E.Z. Cardoso, M.M. Tusi, M. Linardi, E.V. Spinace, A.O. Neto, Int. J. Electrochem. Sci. **6**, 3594–3606 (2011)
11. J.-H. Choi, K.-W. Park, I.-S. Park, K. Kim, J.-S. Lee, Y.-E. Sung, J. Electrochem. Soc. **153**, A1812–A1817 (2006)
12. C. Jin, Y. Song, Z. Chen, Electrochim. Acta **54**, 4136–4140 (2009)
13. J.C.M. Silva, B. Anea, R.F.B. De Souza, M.H.M.T. Assumpcao, M.L. Calegaro, A.O. Neto, M.C. Santos, J. Braz. Chem. Soc. **24**, 1553–1560 (2013)
14. J. Tayal, B. Rawat, S. Basu, Int. J. Hydrog. Energy **36**, 14884–14897 (2011)
15. R. Wang, B. Wei, H. Wang, S. Ji, J. Key, X. Zhang, Z. Lei, Ionics **17**, 595–601 (2011)

16. S.Y. Shen, T.S. Zhao, J.B. Xu, Electrochim. Acta **55**, 9179–9184 (2010)
17. H. Hou, S. Wang, W. Jin, Q. Jiang, L. Sun, L. Jiang, G. Sun, Int. J. Hydrog. Energy **36**, 5104–5109 (2011)
18. T. Herranz, S. García, M.V. Martínez-Huerta, M.A. Peña, J.L.G. Fierro, F. Somodi, I. Borbáth, K. Majrik, A. Tompos, S. Rojas, Int. J. Hydrog. Energy **37**, 7109–7118 (2012)
19. E.V. Spinace, R.R. Dias, M. Brandalise, M. Linardi, A. Oliveira Neto, Ionics **16**, 91–95 (2010)
20. J. Ribeiro, D.M. dos Anjos, K.B. Kokoh, C. Coutanceau, J.M. Léger, P. Olivi, A.R. de Andrade, G. Tremiliosi-Filho, Electrochim. Acta **52**, 6997–7006 (2007)
21. L. Cao, G. Sun, H. Li, Q. Xin, Electrochem. Commun. **9**, 2541–2546 (2007)
22. Q.-Y. Qian, C. Yang, Y.-G. Zhou, S. Yang, X.-H. Xia, J. Electroanal. Chem. **660**, 57–63 (2011)
23. C.-W. Liu, Y.-W. Chang, Y.-C. Wei, K.-W. Wang, Electrochim. Acta **56**, 2574–2581 (2011)
24. A.R. Hind, S.K. Bhargava, A. McKinnon, Adv. Colloid Interface Sci. **93**, 91–114 (2001)
25. S. Song, Y. Wang, P. Shen, Chin. J. Catal. **28**, 752–754 (2007)
26. R.F.B. De Souza, J.C.M. Silva, F.C. Simões, M.L. Calegaro, A.O. Neto, M.C. Santos, Int. J. Electrochem. Sci. **7**, 5356–5366 (2012)
27. A.O. Neto, J. Nandenha, M.H.M.T. Assumpção, M. Linardi, E.V. Spinacé, R.F.B. de Souza, Int. J. Hydrog. Energy **38**, 10585–10591 (2013)
28. S.G. da Silva, J.C.M. Silva, G.S. Buzzo, R.F.B. de Souza, E.V. Spinacé, A.O. Neto, M.H.M.T. Assumpção. Int. J. Hydrogen Energy **39**, 10121–10127 (2014)